Amyloids

International Edition: DOI: 10.1002/anie.201502644
German Edition: DOI: 10.1002/ange.201502644

A Functional Role for Aβ in Metal Homeostasis? N-Truncation and High-Affinity Copper Binding**

Mariusz Mital, Nina E. Wezynfeld, Tomasz Frączyk, Magdalena Z. Wiloch, Urszula E. Wawrzyniak, Arkadiusz Bonna, Carolin Tumpach, Kevin J. Barnham, Cathryn L. Haigh, Wojciech Bal, and Simon C. Drew**

Abstract: *Accumulation of the β-amyloid (Aβ) peptide in extracellular senile plaques rich in copper and zinc is a defining pathological feature of Alzheimer's disease (AD). The Aβ1–x (x = 16/28/40/42) peptides have been the primary focus of Cu^{II} binding studies for more than 15 years; however, the N-truncated Aβ4–42 peptide is a major Aβ isoform detected in both healthy and diseased brains, and it contains a novel N-terminal FRH sequence. Proteins with His at the third position are known to bind Cu^{II} avidly, with conditional log K values at pH 7.4 in the range of 11.0–14.6, which is much higher than that determined for Aβ1–x peptides. By using Aβ4–16 as a model, it was demonstrated that its FRH sequence stoichiometrically binds Cu^{II} with a conditional K_d value of 3×10^{-14} M at pH 7.4, and that both Aβ4–16 and Aβ4–42 possess negligible redox activity. Combined with the predominance of Aβ4–42 in the brain, our results suggest a physiological role for this isoform in metal homeostasis within the central nervous system.*

Alzheimer's disease (AD) is a neurodegenerative condition characterized by progressive cognitive decline and cerebral deposition of fibrillar plaques comprised of the β-amyloid (Aβ) peptide.[1] There is compelling evidence that in AD, the brain undergoes widespread oxidative stress, which has been linked with unusually high concentrations of redox-active transition metals, particularly Cu, within amyloid plaques.[2]

The first protein sequencing studies of the plaque core of AD patients identified a significant proportion of Aβ peptides with "ragged" N termini, with Aβ4–*x* isoforms accounting for more than 60% of brain amyloid.[3,4] More recent mass spectrometry analyses confirmed these seminal findings, demonstrating that Aβ4–42 and Aβ1–42 are the dominant isoforms present in the hippocampus and cortex of sporadic AD patients, as well as in healthy controls.[5,6] Although we have previously noted that Aβ4–*x* peptides contain the amino-terminal copper and nickel (ATCUN, H_2N-Xaa–Yaa–His–) motif,[7] which enables high affinity Cu^{II} binding via a $\{NH_2^{Xaa}, N^{-Yaa}, N^{-His}, N_{Im}^{His}\}$ coordination sphere,[8] interest has remained focused on elucidating the Cu^{II} coordination and affinity of Aβ1–*x* peptides.[9,10]

In this study, we fully characterize the Cu^{II} binding properties of Aβ4–16 by using a range of spectroscopic and potentiometric techniques. We demonstrate that the fused (5,5,6)-membered chelate rings formed by the first three residues of Aβ4–*x* provide a Cu^{II} binding site with a conditional log *K* value more than three orders of magnitude higher than that reported for Aβ1–*x* peptides and thirty times higher than that of human serum albumin (HSA), which also shares the ATCUN motif.[11] The Aβ4–16 peptide contains a second Cu^{II} binding site, fully separated from the N-terminal site, but with an affinity that is lower by seven orders of magnitude.

We began by characterizing the pH dependence of Cu^{II} coordination by Aβ4–16 by UV/Vis, CD, and EPR spectroscopy at a substoichiometric Cu^{II} ratio. The results indicate the presence of a sole spectroscopic species above pH 5

[*] M. Mital,[+] C. Tumpach, K. J. Barnham, S. C. Drew
Florey Department of Neuroscience and Mental Health
The University of Melbourne, Victoria, 3010 (Australia)
E-mail: sdrew@unimelb.edu.au
M. Mital,[+] N. E. Wezynfeld,[+] T. Frączyk, A. Bonna, W. Bal
Institute of Biochemistry and Biophysics
Polish Academy of Sciences, Warsaw (Poland)
E-mail: wbal@ibb.waw.pl
M. Z. Wiloch, U. E. Wawrzyniak
Department of Microbioanalytics, Faculty of Chemistry
Warsaw University of Technology (Poland)
K. J. Barnham
Department of Pharmacology and Therapeutics
The University of Melbourne, Victoria, 3010 (Australia)
C. L. Haigh
Department of Medicine, Royal Melbourne Hospital
The University of Melbourne, Victoria, 3010 (Australia)
[+] These authors contributed equally to this work.

[**] This work was supported by a Future Fellowship (FT110100199) administered by the Australian Research Council (ARC) to S.C.D, an ARC Linkage Infrastructure, Equipment and Facilities grant (LE130100061) to S.C.D. and K.J.B., and a Senior Research Fellowship administered by the National Health and Medical Research Council of Australia to K.J.B. This work was also supported by the Foundation for Polish Science TEAM Program, co-financed from European Regional Development Fund resources within the framework of Operational Program Innovative Economy under the project "Metal-Dependent Peptide Hydrolysis Tools and Mechanisms for Biotechnology, Toxicology and Supramolecular Chemistry" (TEAM 2009-4/1) to W.B. The study was sponsored in part by the National Science Centre of Poland, grant no. 2014/15/B/ST5/05229. The equipment used was sponsored in part by the Centre for Preclinical Research and Technology (CePT), a project cosponsored by the European Regional Development Fund and Innovative Economy, The National Cohesion Strategy of Poland. Electrochemical studies were financially supported by the National Science Center of Poland SONATA project 2012/07/D/ST4/02187.
Supporting information for this article is available on the WWW under http://dx.doi.org/10.1002/anie.201502644.

(Figure 1). Protonation and stability constants for the Cu^{II} complexes of Aβ4–16 calculated from pH-metric titrations are presented in Table 1 (see the Supporting Information for assignments and discussion of the acid/base properties of the peptide). A comparison of p*K* values and spectroscopic parameters (Table 2) with reported data[11–16] clearly indicates the formation of the ATCUN-type complex at the N-terminal FRH sequence under mildly acidic conditions (a CuH_3L^{2+} complex with an apparent p*K* value of 4.1). This species, which contains a deprotonated Asp7 carboxylate, undergoes a series of further deprotonations with increasing pH values (Table 1, Figure 1b). Starting from acidic pH values, these are Glu11 (around pH 5), followed by His13/His14 (pH 6–7), and finally Tyr10 and Lys16 (pH 10.1–10.2). Except for the processes above pH 10, these deprotonations occurred at pH values slightly higher (by 0.4–0.9) than those in the free Aβ4–16 peptide. This effect is due to lower overall charges of the respective Cu^{II} complexes compared with the free peptide species, as indicated in Table 1. A weak fifth coordination site in the N-terminal Cu^{II} complex of Aβ4–16 may be occupied by a water molecule, in a manner analogous to the Cu^{II} complex of the DAHK-am tetrapeptide.[17] Alternatively, the Asp7 side chain may obscure one apical coordination site (Figure 2).

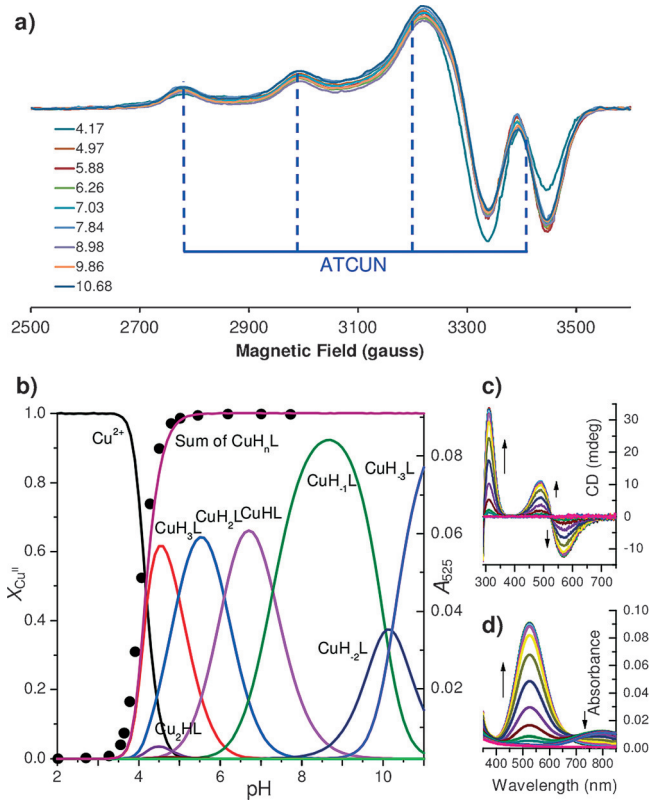

Figure 1. The FRH sequence of Aβ4–16 binds Cu^{II} through the ATCUN motif. a) pH-dependent EPR spectra. Dashed lines in show principal hyperfine ($A_{||}$) features associated with the ATCUN site. b) Species distribution plot. c) CD spectra. d) UV/Vis spectra. Filled circles in (b) compare the pH dependence of the d–d band at 525 nm shown in (d) with the profile of formation of CuH_nL complexes derived from potentiometry. Conditions: 0.9 mM Cu^{II}, 1.0 mM Aβ4–16 (L).

Table 1: Protonation and stability constants (log β values) for Aβ4–16 (L) and its Cu^{II} complexes at $I = 0.1$ M (KNO_3) and 25 °C. Standard deviations on the last digits are given in parentheses.

Species	Log β[a]	pK[b]	Assignment[c]	Coordination Mode
H_8L^{5+}	53.630(6)			
H_7L^{4+}	50.651(5)	2.98	Asp7	
H_6L^{3+}	46.546(5)	4.10	Glu11	
H_5L^{2+}	40.843(5)	5.70	His6/13/14	
H_4L^{+}	34.501(5)	6.34	His6/13/14	
H_3L	27.801(5)	6.70	His6/13/14	
H_2L^{-}	20.188(3)	7.61	Phe4 N-term.	
HL^{2-}	10.297(4)	9.89	Tyr10/Lys16	
L^{3-}		10.30	Lys16/Tyr10	
CuH_3L^{2+}	37.496(5)			4N
CuH_2L^{+}	32.518(8)	4.98	Glu11	4N
CuHL	26.419(9)	6.10	His13/14	4N
CuL^{-}	19.13(1)	7.28	His13/14	4N
$CuH_{-1}L^{2-}$	9.07(2)	10.06	Tyr10/Lys16	4N
$CuH_{-2}L^{3-}$	−1.15(2)	10.22	Lys16/Tyr10	4N
Cu_2HL^{2+}	30.87(1)			4N, 1N
Cu_2L^{+}	25.365(8)	5.50	His13/14	4N, 2N
$Cu_2H_{-1}L$	18.57(1)	6.80	His14 N^{-}	4N, 3N
$Cu_2H_{-2}L^{-}$	10.29(1)	8.28	His13 N^{-}	4N, 3+1N
$Cu_2H_{-3}L^{2-}$	1.03(1)	9.26	Val12 N^{-}	4N, 4+1N
$Cu_2H_{-4}L^{3-}$	−9.11(2)	10.14	Tyr10/Lys16	4N, 4+1N
$Cu_2H_{-5}L^{4-}$	-19.72(2)	10.61	Lys16/Tyr10	4N, 4+1N

[a] $\beta(H_nL) = [H_nL]/([L][H^+])^n$; $\beta(Cu_mH_nL) = [M_mH_nL]/([M]^m[L][H^+]^n)$. [b] Deprotonation to yield the given species. [c] Deprotonated residue (side chain unless marked otherwise).

Table 2: Spectroscopic data for the ATCUN site of Cu(Aβ4–16).

EPR[a]				UV/Vis[b]	CD[b]
$g_{||}$	$g_{\perp}$	$A_{||}$	$A_{\perp}$	λ_{max} (ε)	λ_{ext} ($\Delta\varepsilon$)
2.183(1)	2.043(1)	215(2)	25(2)	525 (100)	570 (−0.40)
					488 (+0.34)
					311 (+1.13)
					287 (−0.52)

[a] Uncertainties in the final digit are given in parentheses. Hyperfine values are for the ^{65}Cu isotope in units of 10^{-4} cm^{-1}. [b] λ [nm], ε [$M^{-1}cm^{-1}$].

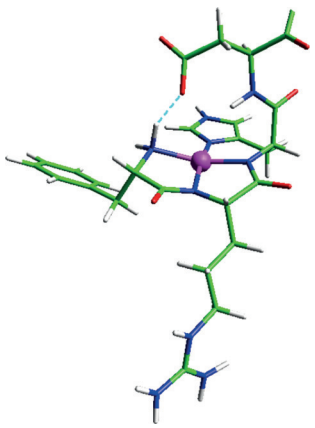

Figure 2. DFT-optimized structure of the ATCUN Cu^{II} binding site of Aβ4–*x*. A possible hydrogen-bonding interaction between Phe4 and Asp7 is indicated (dashed line).

The stabilities of various complexes can be conveniently calculated and compared by using the competitivity index (CI) method.[18,19] The CI, calculated for given concentrations of reagents and pH values, is equivalent to the logarithm of the conditional stability constant at these conditions. Its value for the N-terminal ATCUN site of Aβ4–16 at pH 7.4 is 13.53, which corresponds to a K_d value of 30 fM. This value is in the upper part of the range known for ATCUN sites (11.0–14.6, Table S1 in the Supporting Information).

Potentiometric and spectroscopic titrations performed in the presence of a two-fold excess of Cu^{II} ions demonstrated the formation of another set of complexes that are formed sequentially, that is, only after saturation of the ATCUN site. Analysis of structures and spectroscopic properties of these complexes is given in the Supporting Information. The CI method yielded the logarithm for the conditional constant of the second Cu^{II} ion binding to Aβ4–16 at pH 7.4 as 6.72 (K_d = 0.19 μM). The $Cu_2H_{-1}L$ complex, which contains equatorial coordination of two His imidazole nitrogen atoms and the His14 peptide nitrogen atom, is the major contributor to this affinity (Figure S1 in the Supporting Information).

In order to demonstrate the importance of the amino-terminal aspartate for the binding of Cu^{II} by Aβ1–16, one study has considered the coordination of Aβ4–16;[20] however, this species was deemed physiologically irrelevant and the conditional dissociation constant determined from tyrosine fluorescence was anomalously high owing to a neglect of the inner filter effect.[21] We therefore re-analysed the changes in Tyr10 fluorescence of Aβ4–16 upon Cu^{II} titration. We also carried out a parallel experiment with Aβ1–16. Both peptides exhibited linear fluorescence quenching and show sequential binding of two Cu^{II} equivalents, with K_d values greater than 1 μM (Figure S2 in the Supporting Information). The effect for Aβ1–16 was in full agreement with a previous study demonstrating the unsuitability of this approach for the determination of Cu^{II} affinities for Aβ peptides.[21]

The high affinity of the N-terminal site suggested that Aβ4–*x* should be able to compete successfully with Aβ1–*x* peptides for Cu^{II} ions. We demonstrated this ability directly for the model peptides Aβ4–16 and Aβ1–16 at pH 7.4 by using EPR and UV/Vis spectroscopy (Figure 3). The transfer of Cu^{II} from Aβ1–16 to Aβ4–16 was quantitative and immediate, and no intermediate species could be identified.

Despite the inherently high Cu^{II} binding affinity of peptides containing the ATCUN motif, some have been shown to generate levels of reactive oxygen species (ROS) comparable with unbound Cu^{II} in the presence of ambient O_2.[8,22,23] Using the fluorescent probe 2-[6-(4′-amino)phenoxy-*3H*-xanthen-3-on-9-yl]benzoic acid (APF), we therefore compared the hydroxyl radical production of Aβ4–16 with those of HSA and Aβ1–16 in the presence of substoichiometric Cu^{II} and ascorbate (Figure 4a,b). Cu^{II}(Aβ4–16) was observed to produce a significantly lower level of hydroxyl radicals than Cu^{II}(HSA); in fact, there was no significant difference in hydroxyl radical production by Aβ4–16 in the presence and absence of Cu^{II}. The Aβ1–16 peptide, on the other hand, produced high levels of ROS compared with both Aβ4–16 and the ATCUN binding site of HSA as previously reported.[24]

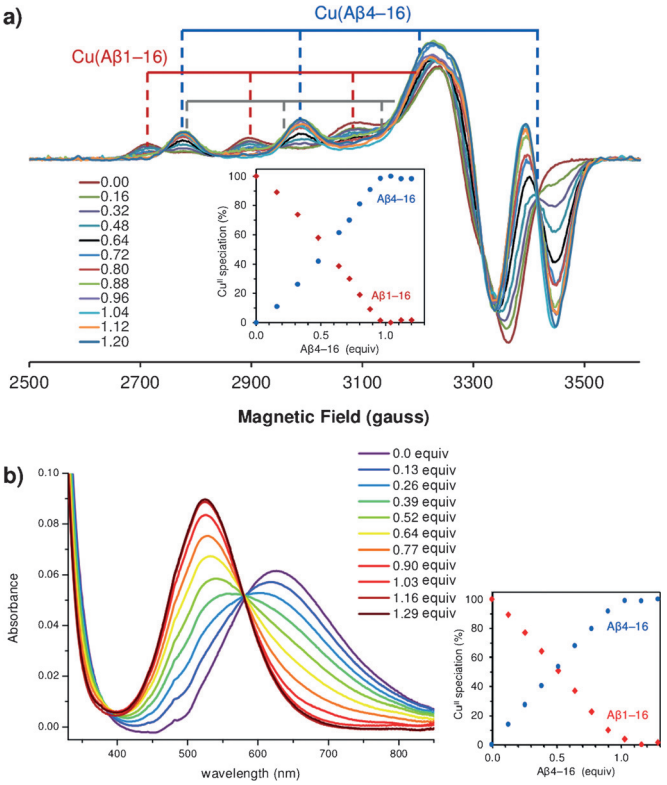

Figure 3. a) X-band (9.45 GHz) EPR and b) UV/Vis spectra showing the exchange of Cu^{II} from Aβ1–16 as Aβ4–16 is titrated into a solution of Cu^{II}/Aβ1–16 0.9:1 in HEPES buffer pH 7.4. Dashed vertical lines in (a) indicate distinguishable features associated with the largest component of the ^{65}Cu hyperfine interaction ($A_{||}$) for each species; the minor species of Cu^{II}(Aβ1–16), "component II", is indicated by gray lines. The insets show speciation diagrams determined from the decomposition of the EPR spectra (Figure S3) and by following the absorption at 632 nm for Aβ1–16 and 525 nm for Aβ4–16.

To ascertain whether physiological Aβ4–42 also demonstrates low ROS production, we repeated the assay with Aβ4–42 and Aβ1–42 (Figure 4c,d). Again, the N-truncated species exhibited negligible hydroxyl radical production compared to Aβ1–42. At the completion of the assay, polyacrylamide gel electrophoresis under mild denaturing conditions indicated retarded electrophoretic mobility for Aβ1–42, which is consistent with oxidative modification as a result of ROS production (Figure S4). In line with the known high aggregation propensity of Aβ4–42,[25] a comparatively low proportion of monomeric Aβ4–42 was evident, thus suggesting that most of the oligomers did not dissociate and enter the gel. Despite the fact that aggregation occurred throughout the assay, Aβ4–42 retained its low redox activity. Hence, while we cannot rule out that some misfolded isoforms of Aβ4–42 have higher redox activity, ROS production appears to be independent of oligomeric state under these specific assay conditions.

The above results demonstrate that Cu^{II}-bound Aβ4–*x* species have low redox activity in terms of the Cu^{I}/Cu^{II} couple, since the function of ascorbate is to reduce Cu^{II}, thereby closing the redox cycle. In order to explain this observation, we performed a series of electrochemical experi-

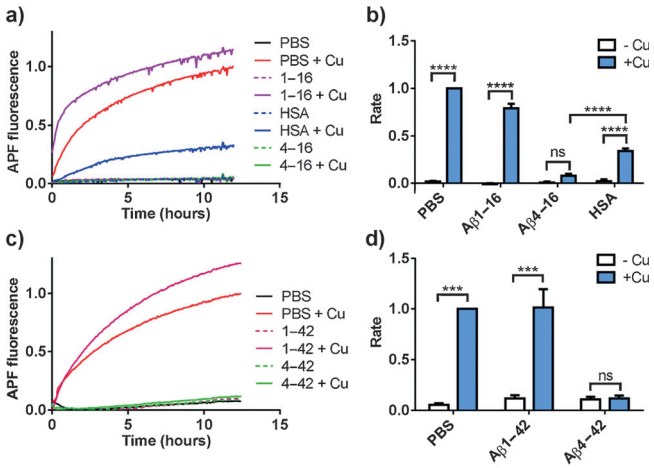

Figure 4. a, c) Representative time traces and b, d) the rate of hydroxyl radical production (between 3—12 h) by Aβ peptides and HSA, with and without Cu^{II}, as measured by APF fluorescence. No significant differences between the samples were observed in the absence of Cu^{II}. The addition of $CuCl_2$ led to significant hydroxyl radical production in all of samples except Aβ4–16 and Aβ4–42, the results for which were not significantly different from those with buffer alone. Conditions: [Aβ] = [HSA] = 10 μM, [Cu^{II}] = 0 or 9 μM, [APF] = 100 μM, [Asc] = 300 μM, [phosphate] = 10 mM, pH 7.2. ***$p < 0.001$, ****$p < 0.0001$, ns = not significant. The curves in (a, c) and ROS production rates in (b, d) were normalized to the PBS + Cu condition.

ments on Aβ4–16 in the presence of one or two Cu^{II} equivalents at pH 6.8 and 7.4. Cyclic voltammetry (CV) and two pulse techniques (differential pulse voltammetry (DPV) and square wave voltammetry (SWV)) were employed for this purpose. CV scans of the peptide alone and its complexes in water solution are shown in Figure 5 (for DPV and SWV, see Figure S5). For the peptide alone, the main anodic irreversible peak was observed at 0.67(2) V for both pH values. This potential corresponds to oxidation of the Tyr 10 phenol ring. The mechanism, well known for carbon electrodes, involves the formation of a thermodynamically unstable radical, which is converted into an electroactive orthoquinone.[26,27]

In contrast to Cu^{II}(Aβ1–16),[28] the ATCUN Cu^{II} complex of Aβ4–16, which is solely present at a metal-to-peptide ratio of 0.9:1 for both pH 6.8 and 7.4, yielded no electrochemical

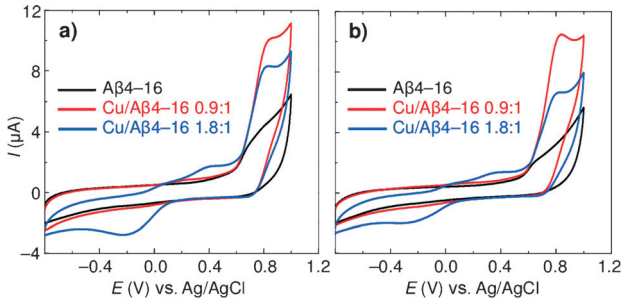

Figure 5. Cyclic voltammetry scans of Aβ4–16 and its Cu^{II} complexes at pH 6.8 (a) and pH 7.4 (b), recorded in 96 mM KNO_3/4 mM HNO_3, $\nu = 0.1\ Vs^{-1}$.

activity that could be assigned to a Cu^{I}/Cu^{II} redox couple. The main peaks at 0.85 V (pH 6.8) and 0.83 V (pH 7.4) vs. Ag/AgCl are associated with the irreversible oxidation of Cu^{II} to Cu^{III}. The CV curves obtained in the presence of a second Cu^{II} ion exhibited additional peaks at less positive potentials, which is indicative of the Cu^{I}/Cu^{II} couple. As before, an irreversible anodic response, associated with the formation of Cu^{III}, appeared at 0.82 V. However, the corresponding oxidation current was lower at both pH values.

Taken together, these observations present a clear picture of a highly ordered metal binding site of low redox activity within an otherwise disordered peptide. This contrasts with the general classification of Aβ as an intrinsically-disordered metalloprotein, the low Cu^{II} affinity of which relative to classical cuproproteins renders it incapable of binding Cu^{II} except during conditions of metal dysregulation.[10] The conditional binding constant determined here for Aβ4–16 is three orders of magnitude higher than that determined for Aβ1–*x*. Coupled with the repeated findings that Aβ4–42 is a dominant Aβ isoform even in the healthy brain,[5,6] we therefore postulate a hitherto unforeseen role for Aβ in metal homeostasis in the central nervous system.

Keywords: Alzheimer's disease · amyloid · bioinorganic chemistry · copper · peptides

How to cite: *Angew. Chem. Int. Ed.* **2015**, *54*, 10460–10464
Angew. Chem. **2015**, *127*, 10606–10610

[1] C. L. Masters, D. J. Selkoe, *Cold Spring Harbor Perspect. Med.* **2012**, *2*, a006262.
[2] K. J. Barnham, A. I. Bush, *Curr. Opin. Chem. Biol.* **2008**, *12*, 222–228.
[3] C. L. Masters, G. Simms, N. A. Weinman, G. Multhaup, B. L. McDonald, K. Beyreuther, *Proc. Natl. Acad. Sci. USA* **1985**, *82*, 4245–4249.
[4] C. L. Masters, G. Multhaup, G. Simms, J. Pottgiesser, R. N. Martins, K. Beyreuther, *EMBO J.* **1985**, *4*, 2757–2763.
[5] H. Lewis, D. Beher, N. Cookson, A. Oakley, M. Piggott, C. M. Morris, E. Jaros, R. Perry, P. Ince, R. A. Kenny, C. G. Ballard, M. S. Shearman, R. N. Kalaria, *Neuropathol. Appl. Neurobiol.* **2006**, *32*, 103–118.
[6] E. Portelius, N. Bogdanovic, M. K. Gustavsson, I. Volkmann, G. Brinkmalm, H. Zetterberg, B. Winblad, K. Blennow, *Acta Neuropathol.* **2010**, *120*, 185–193.
[7] S. C. Drew, C. J. Noble, C. L. Masters, G. R. Hanson, K. J. Barnham, *J. Am. Chem. Soc.* **2009**, *131*, 1195–1207.
[8] C. Harford, B. Sarkar, *Acc. Chem. Res.* **1997**, *30*, 123–130.
[9] S. C. Drew, K. J. Barnham, *Acc. Chem. Res.* **2011**, *44*, 1146–1155.
[10] P. Faller, C. Hureau, G. La Penna, *Acc. Chem. Res.* **2014**, *47*, 2252–2259.
[11] M. Rózga, M. Sokołowska, A. M. Protas, W. Bal, *J. Biol. Inorg. Chem.* **2007**, *12*, 913–918.
[12] W. Bal, J. Christodoulou, P. J. Sadler, A. Tucker, *J. Inorg. Biochem.* **1998**, *70*, 33–39.
[13] W. Bal, M. Jeżowska-Bojczuk, K. S. Kasprzak, *Chem. Res. Toxicol.* **1997**, *10*, 906–914.
[14] M. Sokołowska, A. Krężel, M. Dyba, Z. Szewczuk, W. Bal, *Eur. J. Biochem.* **2002**, *269*, 1323–1331.
[15] H. F. Stanyon, X. Cong, Y. Chen, N. Shahidullah, G. Rossetti, J. Dreyer, G. Papamokos, P. Carloni, J. H. Viles, *FEBS J.* **2014**, *281*, 3945–3954.
[16] H. Sigel, R. B. Martin, *Chem. Rev.* **1982**, *82*, 385–426.

[17] C. Hureau, H. Eury, R. Guillot, C. Bijani, S. Sayen, P.-L. Solari, E. Guillon, P. Faller, P. Dorlet, *Chem. Eur. J.* **2011**, *17*, 10151 – 10160.
[18] A. Krężel, J. Wójcik, M. Maciejczyk, W. Bal, *Chem. Commun.* **2003**, 704 – 705.
[19] I. Zawisza, M. Rózga, W. Bal, *Coord. Chem. Rev.* **2012**, *256*, 2297 – 2307.
[20] J. W. Karr, H. Akintoye, L. J. Kaupp, V. A. Szalai, *Biochemistry* **2005**, *44*, 5478 – 5787.
[21] B. Alies, E. Renaglia, M. Rózga, W. Bal, P. Faller, C. Hureau, *Anal. Chem.* **2013**, *85*, 1501 – 1508.
[22] M. D. Libardo, J. L. Cervantes, J. C. Salazar, A. M. Angeles-Boza, *ChemMedChem* **2014**, *9*, 1892 – 1901.
[23] W. Bal, J. Lukszo, K. S. Kasprzak, *Chem. Res. Toxicol.* **1997**, *10*, 915 – 921.
[24] L. Perrone, E. Mothes, M. Vignes, A. Mockel, C. Figueroa, M. C. Miquel, M. L. Maddelein, P. Faller, *ChemBioChem* **2010**, *11*, 110 – 118.
[25] Y. Bouter, K. Dietrich, J. L. Wittnam, N. Rezaei-Ghaleh, T. Pillot, S. Papot-Couturier, T. Lefebvre, F. Sprenger, O. Wirths, M. Zweckstetter, T. A. Bayer, *Acta Neuropathol.* **2013**, *126*, 189 – 205.
[26] T. A. Enache, A. M. Oliveira-Brett, *J. Electroanal. Chem.* **2011**, *655*, 9 – 16.
[27] T. A. Enache, A. M. Oliveira-Brett, *Bioelectrochemistry* **2013**, *89*, 11 – 18.
[28] C. Hureau, V. Balland, Y. Coppel, P. L. Solari, E. Fonda, P. Faller, *J. Biol. Inorg. Chem.* **2009**, *14*, 995 – 1000.

Received: March 22, 2015
Published online: July 14, 2015

